Published online 16 August 2010 Nucleic Acids Research, 2010, Vol. 38, No. 22 8061–8071
doi:10.1093/nar/gkq717

AUF1 p42 isoform selectively controls both steady-state and PGE_2-induced *FGF9* mRNA decay

Tsung-Ming Chen[1], Chien-Hui Hsu[2], Shaw-Jenq Tsai[1,3,*] and H. Sunny Sun[1,2,*]

[1]Institute of Basic Medical Sciences, [2]Institute of Molecular Medicine and [3]Department of Physiology, National Cheng Kung University Medical College, Tainan, Taiwan

Received May 6, 2010; Revised July 7, 2010; Accepted July 28, 2010

ABSTRACT

Fibroblast growth factor 9 (FGF9) is an autocrine/paracrine growth factor that plays vital roles in many physiologic processes including embryonic development. Aberrant expression of FGF9 causes human diseases and thus it highlights the importance of controlling FGF9 expression; however, the mechanism responsible for regulation of FGF9 expression is largely unknown. Here, we show the crucial role of an AU-rich element (ARE) in *FGF9* 3′-untranslated region (UTR) on controlling FGF9 expression. Our data demonstrated that AUF1 binds to this ARE to regulate *FGF9* mRNA stability. Overexpression of each isoform of AUF1 (p37, p40, p42 and p45) showed that only the p42 isoform reduced the steady-state *FGF9* mRNA. Also, knockdown of $p42^{AUF1}$ prolonged the half-life of *FGF9* mRNA. The induction of FGF9 mRNA in prostaglandin (PG) E_2-treated human endometrial stromal cells was accompanied with declined cytoplasmic AUF1. Nevertheless, ablation of AUF1 led to sustained elevation of FGF9 expression in these cells. Our study demonstrated that $p42^{AUF1}$ regulates both steady-state and PGE_2-induced *FGF9* mRNA stability through ARE-mediated mRNA degradation. Since almost half of the FGF family members are ARE-containing genes, our findings also suggest that ARE-mediated mRNA decay is a common pathway to control *FGFs* expression, and it represents a novel RNA regulon to coordinate *FGFs* homeostasis in various physiological conditions.

INTRODUCTION

The mammalian fibroblast growth factor (FGF) family includes 18 distinct members and are grouped into six subfamilies based on the differences in sequence homology and phylogeny [review see (1)]. Many of these FGFs are expressed abundantly in a specific spatial and temporal pattern and considered to play substantial roles in development (2), angiogenesis (3), hematopoiesis (4) and tumorigenesis (5). Human fibroblast growth factor 9 (FGF9; MIN# 600921) shares >93% sequence identity with *Xenopus*, mice and rats (6,7), suggesting that FGF9 is important and may have similar functions across species. Previous studies suggested that FGF9 functions as an autocrine/paracrine growth factor for neuron cells (8), fibroblasts (9) and endometrial stromal cells (10), and as an oncogene for NIH3T3 fibroblast cells (11).

FGF9 mRNA is ubiquitously expressed in the embryo but is restricted to kidney, brain and uterus in the adult (10–12). Furthermore, abnormal expression of FGF9 is involved in several human diseases, including cancer (13,14), endometriosis (15), neuron degeneration (16), male-to-female sex reversal (17) and male infertility (18). Nevertheless, upon stimulation by factors like prostaglandin (PG) E_2 (19), estrogen (10), androgen (20) and retinoic acid (21), the mRNA of *FGF9* is upregulated but rapidly returns to basal levels. These studies implied that the expression of FGF9 needs to be strictly controlled. While the functions of FGF9 in physiological and pathological processes are well studied, mechanisms that control steady-state and stimuli-induced *FGF9* mRNA levels to maintain FGF9 homeostasis remain largely unknown.

Regulation of the rate of mRNA decay is an important mechanism to control gene expression at the post-transcriptional level (22). The interaction between *cis*-acting elements in the transcripts and sequence-specific RNA-binding proteins permits precise control of the mRNA level and, subsequently, the protein level (23). Adenylate/uridylate-rich elements (AREs) are regulatory elements present in the 3′-untranslated region (UTR) of certain mRNAs that have been implicated in post-transcriptional gene regulation by mediating rapid degradation of target mRNA (24,25). AREs are generally found in transcripts that need to be precisely controlled, such as genes that function as growth factors, proto-oncogenes

*To whom correspondence should be addressed. Tel: 886 6 2353535 ext. 3648; Fax: 886 6 2095845; Email: hssun@mail.ncku.edu.tw
Correspondence may also be addressed to Shaw-Jenq Tsai. Tel: 886 6 2353535 ext. 5426, Fax: 886 6 2362780; Email: seantsai@mail.ncku.edu.tw

© The Author(s) 2010. Published by Oxford University Press.
This is an Open Access article distributed under the terms of the Creative Commons Attribution Non-Commercial License (http://creativecommons.org/licenses/by-nc/2.5), which permits unrestricted non-commercial use, distribution, and reproduction in any medium, provided the original work is properly cited.

and cytokines (23,26,27). At least 17 *trans*-acting factors have been identified (28) to interact with mRNA containing AREs. Most of these proteins, such as the AU-rich element-binding protein 1 (AUF1) family (29), the tristetraprolin (TTP) family (30) and the KH-type splicing regulatory protein (KSRP) (31) reduce the target mRNA level. In contrast, factors like human antigen R (HuR) positively regulate target gene expression (32).

We previously reported that a microsatellite motif in the 3′-UTR of the *FGF9* gene is important for controlling the mRNA stability of *FGF9* (17). The work demonstrated a new post-transcriptional regulation of FGF9 expression and suggested the expression of *FGF9* may be controlled by a network that involves multiple layers of regulations. In this study, we set out to investigate other novel mechanisms responsible for the tight regulation of *FGF9* mRNA stability.

MATERIALS AND METHODS

Cell culture

A human embryonic kidney cell line HEK293 expressing endogenous FGF9 was grown in minimum essential medium (MEM) (Gibco, Carlsbad, CA, USA) with 10% heat-inactivated horse serum and 1.0 mM sodium pyruvate. Stromal cells were cultured in DMEM/F12 with 10% fetal bovine serum (FBS). In both cases, media were supplemented with 100 U/ml penicillin and 100 μg/ml streptomycin (Invitrogen, Carlsbad, CA, USA). Cells were routinely maintained at 37°C in a humidified 5% CO_2 incubator. For PGE_2 treatment (Cayman Chemical, Ann Arbor, MI, USA), phenol red-free DMEM/F12 medium was supplemented with 1% charcoal-stripped FBS and 1μM PGE_2. Cells infected by shAUF1 and null virus were exposed to 1 μM PGE_2 for the indicated durations. In parallel, the same amount of ethanol was used as control.

Plasmids

The entire *FGF9* 3′-UTR sequence was amplified using forward primer (FGF9 3′-FUTR-F: 5′-GCTCTAGA GCGGACAAAGACAGTTTCTTCACT-3′) and reverse primer (FGF9 3′-FUTR-R1: 5′-GCTCTAGAGCTTTG GAATTTCTATAAATAAATTTAAC-3′) anchored with XbaI restriction enzyme cutting sites. These XbaI polymerase chain reaction (PCR) products were ultimately subcloned into the XbaI site of the pGL3-promoter (pGL3-p) vector containing a SV40 promoter upstream of the firefly luciferase gene (Promega, Madison, WI, USA). The deletion and mutation constructs were generated by the same strategy with different reverse primers. FGF9 3′-UTR 549R (5′-GCTCTAGACTAAG AGGTCTTTGCTTTAAG-3′) and FGF9 3′-FUTR-mut-R1 (5′-GCTCTAGAGCTTTGGAATTTCTATCCCTCC CTTTAAC-3′) were used for the delARE and mutARE constructs, respectively. All constructs were confirmed by direct sequencing.

For AUF1 overexpression, the cDNA of AUF1 was amplified with AUF1CDS-1 (5′-TTTTTAAGCTTTGCT GCTAGTTTCGGTTCG) and AUF1CDS-2 (CCCGCTC GAGGTATGGTTTGTAGCTATTTTG) primers anchored with restriction enzyme cutting sites HindIII and XhoI (indicated by underline) on each 5′-end, respectively. The PCR products were digested by HindIII and XhoI enzymes and cloned into pcDNA3.1/Myc_His(+)A vector (Invitrogen).

Transient transfection and luciferase reporter assay

HEK293 cells were seeded on each well of a 24-well tissue culture plate (2.5×10^5 cells/well) (TPP AG, Trasadingen, Switzerland) and transfected with each plasmid construct (0.5 μg) plus plasmids carrying renilla luciferase as an internal control. The transfection was carried out with Lipofectamine 2000 (Invitrogen) according to the manufacturer's instructions. Cells were incubated for 24 h and harvested by adding 100 μl of reporter lysis buffer (Luciferase Assay System; Promega). The activity of luciferase was measured using a luminometer (Lumat LB 9507; EG&G Berthold, Bad Wildbad, Germany). Firefly luminescence was normalized to the protein concentration. Results are presented relative to normalized luminescence driven from pGL3-promoter and reported as relative luciferase units (RLU). All experiments were done in triplicate and independently performed at least three times.

mRNA isolation and half-life measurement

Total RNA from cells was isolated with the RNeasy mini kit (Qiagen, Hilden, Germany). For RNA half-life measurements of luciferase mRNA, HEK293 cells were transfected with 2.5 μg plasmid/10^6 cells in 6-well plates using Lipofectamine 2000. Twelve hours later, the cells were treated with 5 μg/ml actinomycin D (Act D) (Sigma, St Louis, MO, USA). RNA was extracted from cells treated with Act D at 0, 2, 4, 6 and 8 h for RNA half-life measurement. As for FGF9 mRNA half-life measurement, HEK293 cells were transfected with 40 nM siRNA/10^6 cells in 6-well plates using Lipofectamine 2000. Act D was added and RNA was isolated at 0, 10, 20, 30, 60 and 120 min after treatment. Complementary DNA was synthesized from 2 μg of DNase-treated total RNA using random primers and an ABI RT kit (Apply Biosystems, Forster city, CA, USA).

Real-time PCR measurements were carried out with the Applied Biosystem GeneAmp 7900. This assay was performed with 40 ng of RNA equivalent cDNA in triplicate on an ABI 7900HT Sequence Detection System and analyzed with SDS2.1 software (Apply Biosystems). TaqMan formulations were used and modified by validating the efficiency between target and reference genes according to the manufacturer's protocols (Apply Biosystems). Luciferase TaqMan assays were performed with the primer set pGL3-Luc-1512F (5′-GC GTTATTTATCGGAGTTGCAGTTG-3′)/pGL3-Luc-1512R (5′-CATACTGTTGAGCAATTCACGTTCA-3′) and detected with pGL3-Luc-1512-Probe (5′-(FAM) CC GCGAACGACATTT (TAMRA)-3′) from the Assays-by-Design^{SM} service (Apply Biosystems). FGF9 TaqMan assays were performed with primer set (HS00181829-ml FGF9). Ribosomal 18s (4319413E) (Apply Biosystems)

was used as endogenous control. The comparative C_T method was used to calculate the relative amount of each sample according to the previous description. Finally, the mRNA half-life was determined by linear regression analysis.

UV crosslink and biotin pull-down assay

RNA–protein-binding reactions were performed using 3–5 μg of cytoplasmic extract, 5 μg of recombinant AUF1 (p45 isoform) purchased from USBiological (Swampscott, MA, USA), 10 ng biotin-labeled RNA and 2 μg tRNA, in a final volume of 20 μl using Binding Buffer A [20 mM HEPES-KOH at pH 7.5, 2.5 mM magnesium chloride ($MgCl_2$), 100 mM potassium chloride (KCl), 20% glycerol, 0.5 mM dithiothreitol and protease inhibitor tablets]. Heparin was added at 0.25 μg/μl. Addition of heparin up to 0.75 mg/ml did not have any significant influence on the pattern of UV cross-linking. Reaction mixtures were incubated for 1 h at 37°C and UV irradiated at 254 nm for 20 min (Stratagene, La JoUa, CA, USA) on ice. The samples were analyzed by 10% SDS–PAGE and detected by western analysis.

For biotin pull-down analysis, 200 μg of whole-cell lysates were incubated with 2 μg purified biotinylated riboprobes (FGF9 ARE: Biotin-AAAUUUAUUUAUA; FGF9 mutant ARE: Biotin-AAAGGGAGGGAUA; Dharmacon Research) for 1 h at 25°C. Complexes were isolated with paramagnetic streptavidin-conjugated Dynabeads (Invitrogen), the unbound proteins were removed, and after extensive washes with the binding buffer, the proteins were step-eluted with protein sample buffer. The eluted proteins were then analyzed by western blot analysis.

Western blot analysis

Whole-cell lysates were obtained by RIPA lysis buffer [50 mM KCl, 5% (v/v) glycerol, 0.1% (v/v) Nonidet P-40, 1 mM $MgCl_2$, 1 mM dithiothreitol, 10 mM Tris/HCl pH 8.0]. Nucleus and cytoplasmic fraction were isolated by NE-PER kit (Thermo, Waltham, MA, USA). Protein concentration was determined by the Bradford assay (Bio-rad, Hercules, CA, USA). After protein quantification, equal amounts of whole-cell lysates were boiled in 4% sodium dodecyl sulfate (SDS) sample buffer (250 mM Tris–HCl, 20% 2-mercaptoethanol, 8% SDS, 40% glycerol and 0.02% bromophenol blue) and subjected to SDS-PAGE separation. Proteins were transferred onto polyvinylidene difluoride membrane (Amersham, Buckinghamshire, UK) and detected by an enhanced chemiluminescence (ECL) kit (Amersham). Endogenous AUF1 was detected by polyclonal rabbit anti-mouse AUF1 antiserum (Upstate Biotechnology, Charlottesville, VA, USA) at 1:4000 dilutions. Various recombinant AUF1 isoforms were detected by rabbit monoclonal anti-myc antibody at 1:2000 dilutions. α-Tubulin was used as an internal control and detected by rabbit monoclonal anti-α-tubulin antibody (Cell Signaling Technologies, Beverly, MA, USA) at 1:2000 dilutions. Lamin A/C was used as loading control for nucleus fraction and detected by mouse monoclonal anti-lamin A/C antibody at 1:200 dilutions. (Santa Cruz Biotech, Santa Cruz, CA, USA).

RNA interference

Small interfering RNAs (siRNA) targeting AUF1 and scrambled control duplexes (Invitrogen) were transfected into HEK293 cells with Lipofectamine 2000 (Invitrogen). After 48 h, total protein was isolated and analyzed by western blot analysis. The knockdown efficiency was calculated by normalizing to the signal intensity first to α-tubulin, and then divided by the value of scramble control. For knockdown of AUF1 in stromal cells, plasmids encoding shRNA that targeted all four AUF1 isoforms were transfected into 293T cells to generate shAUF1 lentivirus. Plasmid without any shRNA (Null) was used as a mock control in this experiment. The lentiviral shRNA clones were from the National RNAi Core Facility of Academic Sinica, Taiwan. Stromal cells were infected with Null (pLK0.1) lentivirus, or AUF1 shRNA lentivirus.

Computational analysis of *FGF9* 3′-UTR sequences

Sequences of *FGF9* from the species *Homo sapiens* (Human; NM_002010), *Canis lupus familiaris* (dog; CF406880), *Bos taurus* (cow; DT899064.1), *Sus scrofa* (swine; EW180881), *Taeniopygia guttata* (bird; EH120653), *Mus musculus* (mouse; AA623627) and *Rattus norvegicus* (rat; DV717281) were downloaded from NCB1 CoreNucleotide and aligned with a multiple sequence alignment program (http://searchlauncher.bcm.tmc.edu/ multi-align/multi-align.html). Images of multiple sequence alignment were output by BOXSHADE (http://www.ch.embnet.org/software /BOX_form.html). In addition, conserved *cis*-elements of *FGF9* 3′-UTR were screened by UTRdb (33) and UTRscan (34).

Statistical analysis

All the data sets were analyzed using GraphPad Prism 4.0 (GraphPad Software, Inc., San Diego, CA, USA) and presented as mean ± SEM. Results were further analyzed using one-way analysis of variance (ANOVA), and post-test was processed using Tukey's multiple comparison tests or the Student's *t*-test.

RESULTS

The 3′-UTR of *FGF9* mRNA contains AU-rich elements

To identify potential factors that regulate *FGF9* gene expression post-transcriptionally, we used bioinformatic tools to search for putative regulatory elements in the human *FGF9* 3′-UTR. Beside the $(GA)_n$ and $(TG)_n$ microsatellite motifs we previously reported (17), an ARE located at 593–601 bp downstream of the stop codon was identified (Figure 1A). Similar ARE motifs were also identified in *FGF9* of mouse, rat, cow, dog, swine and distantly related vertebrate, bird. When these ARE sequences were aligned with that found in the human, the result showed 79% and 100% identities in the AU-rich region and the core nonamer, respectively

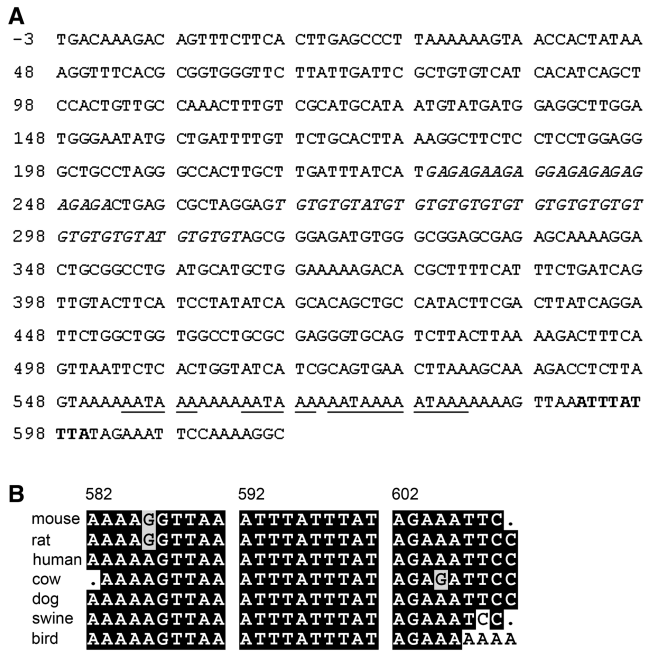

Figure 1. Sequence features of the human *FGF9* 3′-UTR. (**A**) The sequence corresponding to the 3′-UTR of *FGF9* is depicted. The initial TGA nucleotide sequence (−3 to −1) corresponds to the translation stop codon. The GA and TG microsatellite motifs are marked in italic type. The ARE sequence (ATTTATTTA) is marked in bold and the underlines mark the poly-A signals (AATAAA). (**B**) Cross-species alignment of mouse, rat, human, cow, dog, swine and bird showed an overall 79% identity in the AU-rich element region.

(Figure 1B). These results demonstrated that the ARE in the 3′-UTR of human *FGF9* is evolutionarily conserved and suggested that it may play a functional role in controlling the level of *FGF9* mRNA.

ARE is a destabilization element

To functionally characterize the effects of *FGF9* 3′-UTR ARE on regulating *FGF9* expression, sequences containing full-length *FGF9* 3′-UTR (FGF93′-UTR), *FGF9* 3′-UTR with ARE deleted (delARE) and full length with site-directed mutated ARE (mutARE) were cloned into the 3′-UTR of a firefly luciferase reporter construct driven by an SV40 promoter (Figure 2A). Results from the reporter assays showed that the luciferase activities of delARE and mutARE constructs were increased ~1.8- ($P < 0.001$) and 2-fold ($P < 0.001$), respectively, compared with the construct having full-length *FGF9* 3′-UTR (Figure 2B). This result indicates that the ARE is a functional *cis*-element of *FGF9* mRNA and its presence may cause mRNA degradation.

Next, we tested whether ARE affects the mRNA stability by transfecting FGF93′-UTR, delARE and mutARE constructs into HEK293 cells and treating them with 5 μg/ml actinomycin D to inhibit nascent RNA transcription. After quantification by reverse transcription real-time PCR (RT-qPCR), the half-life of each fusion mRNA was determined by linear regression analysis. Our data showed that the fusion mRNA with full-length

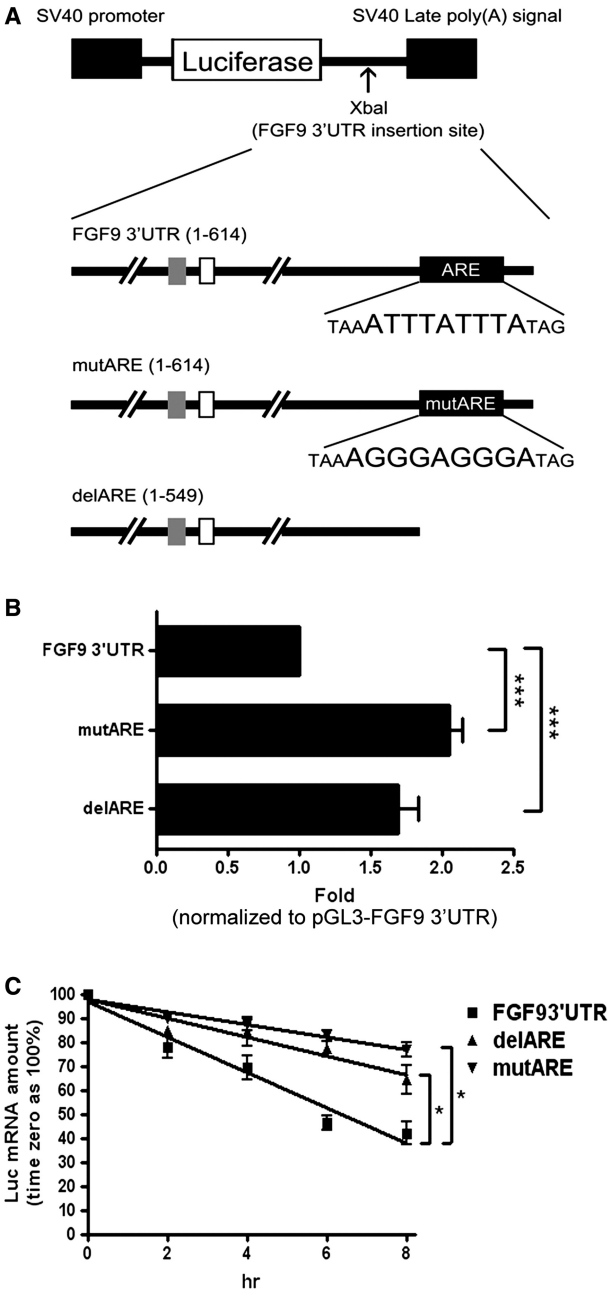

Figure 2. *FGF9* ARE decreases gene expression in HEK293 cells. (**A**) Diagrams showing the firefly luciferase reporter gene construct (top diagram), full-length FGF9 3′-UTR cloned into the 3′-end of the firefly luciferase reporter gene (second diagram), and constructs containing site-direct mutation of ARE (mutARE) (third diagram) and deletion of ARE (delARE) (fourth diagram). Empty and gray squares represent TG and GA dinucleotide repeats, respectively. The black square represents ARE motif. (**B**) Reporter gene activity shown as relative luciferase activity (fold) normalized to FGF9 3′-UTR. (**C**) Effect of FGF9 ARE on mRNA stability detected by real-time RT-qPCR. FGF9 3′-UTR (filled square), delARE (Filled triangle) or mutARE (filled inverted triangle) was transfected into HEK293 cells, which were treated with Act D (5 μg/ml) to inhibit transcription of the luciferase reporter gene. Results are normalized to time zero for each construct. All data are shown as mean ± SEM of 4–6 independent experiments. $^{*}P < 0.05$; $^{***}P < 0.001$.

FGF9 3′-UTR has the shortest half-life ($t_{1/2}$) of 6.98 ± 0.10 h (Figure 2C). In contrast, fusion mRNAs with either deleted or mutated FGF9 ARE significantly prolong the mRNA stability to 9.94 ± 0.13 ($P < 0.05$) or 16.34 ± 0.05 h ($P < 0.05$; Figure 2C). These results demonstrated that *FGF9* ARE is required to reduce the half-life of fusion transcripts.

AUF1 specifically binds to *FGF9* ARE

To determine whether *FGF9* ARE can form protein–RNA complex, we performed UV cross-linking assays and detected three major bands corresponding to molecular masses of ~37, 45 and 55 kDa in whole-cell extracts (Figure 3A). Competition assays showed that these three interacting complexes were quenched with specific cold probes (Figure 3A, left), but not with non-specific ones (Figure 3A, right). These data indicated the proteins are specifically binding to FGF9 ARE.

Since the molecular weights of the proteins binding to *FGF9* ARE are similar to those of AUF1, we set out experiments to test whether AUF1 is the binding protein of *FGF9* ARE. Commercially purified AUF1 protein was

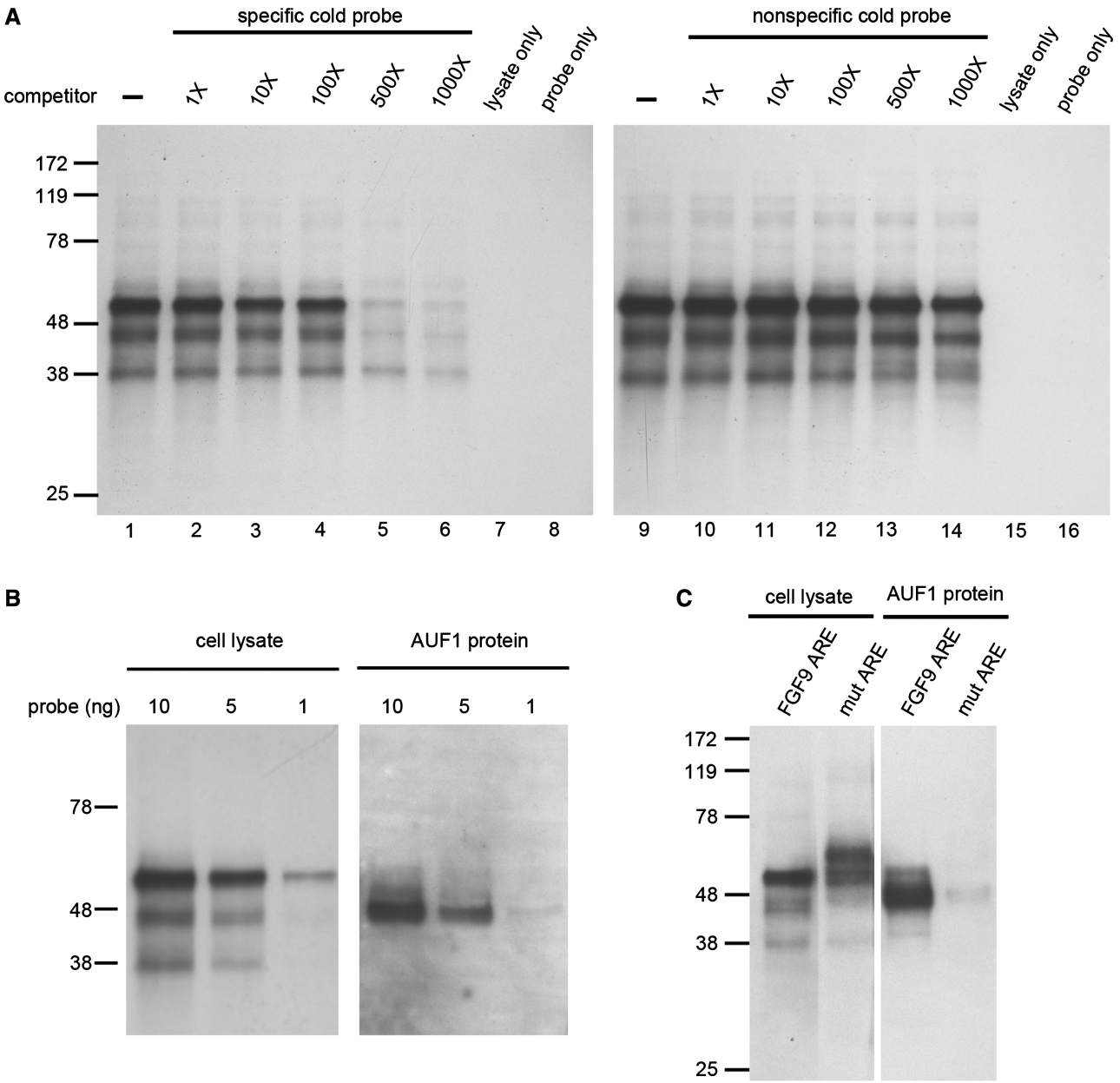

Figure 3. AUF1 specifically binds to *FGF9* 3′-UTR ARE. (**A**) UV cross-linking to biotin-labeled riboprobe from whole-cell lysate of HEK293 cells showed three protein–RNA complexes. Competition assays were performed by adding extra non-biotin-label (cold) riboprobe as competitor with labeled probe. Left panel, specific cold probe; right panel, non-specific cold probe. (**B**) Dose-dependence of proteins in cell lysate (left panel) and AUF1 (right panel) binding to *FGF9* ARE. (**C**) UV cross-linking in cell lysate (left panel) and AUF1 protein (right panel) showing linkage to proteins in the wild-type *FGF9* ARE but not to the mutant ARE.

used in parallel with cell lysate to interact with *FGF9* RNA probe. The AUF1–*FGF9* complex showed a migration rate similar to the 45-kDa complex protein and the protein–RNA binding seems to be dose dependent (Figure 3B). Furthermore, using the mutant probe with a sequence change from AUUUAUUUA to AGGGAG GGA, the protein–RNA complexes located at 37–45 kDa disappeared, while a new complex with molecular mass of ~60 kDa was shown (Figure 3C, left). Interestingly, the AUF1–*FGF9* complex showed a migration rate similar to the 45-kDa complex protein and the protein–RNA binding seems to be abolished when the mutant probe was applied in the reaction (Figure 3B, right). Taken together, these data demonstrated that AUF1 specifically binds to *FGF9* ARE and the molecular weight of AUF1–protein complex is ~45 kDa.

AUF1 knockdown increases *FGF9* mRNA level

To determine the effect of AUF1 on regulation of *FGF9* mRNA, synthetic siRNAs were used to knockdown the endogenous AUF1 in HEK293 cells. Among three exon-specific siRNAs tested, the use of AUF1 exon 1-specific siRNA resulted in the best knockdown effect (Supplementary Figure S1) and was applied in the experiments thereafter. As shown in Figure 4A, compare to the scramble (SC) and AUF1-specific siRNA controls (AC), the AUF1 exon 1-specific siRNA commonly knockdown all 4 AUF1 isoforms. Knocking down AUF1 showed a 2.5-fold increase in luciferase reporter activity in the presence of *FGF9* ARE ($P < 0.01$; Figure 4B). In contrast, the mutARE reporter construct was not affected by AUF1 knockdown indicating the specificity of the AUF1 effect (Figure 4B). Furthermore, knocking down AUF1 also significantly increased endogenous *FGF9* mRNA level to almost 2-fold ($P < 0.01$; Figure 4C). Using RNA stability assays, our data demonstrated that the half-life of endogenous *FGF9* mRNA indeed extended from 19.5 to 60.2 min in AUF1-depleted cells ($P < 0.001$; Figure 4D). Collectively, these data strongly suggest that AUF1 is involved in the destabilization of human *FGF9* transcripts.

$p42^{AUF1}$ overexpression decreases *FGF9* mRNA level

Finally, we determined whether overexpression of AUF1 has the opposite effect on *FGF9* mRNA stability. A biotin pull-down assay was carried out to test the interaction between *FGF9* ARE and AUF1. As expected, AUF1 was specifically interacted with *FGF9* ARE sequence, especially the p42 isoform. Moreover, mutation of the core sequence from U to G resulted in a decrease of the binding affinity to <20% (Figure 5A). To study the isoform-specific interaction between *FGF9* ARE and AUF1

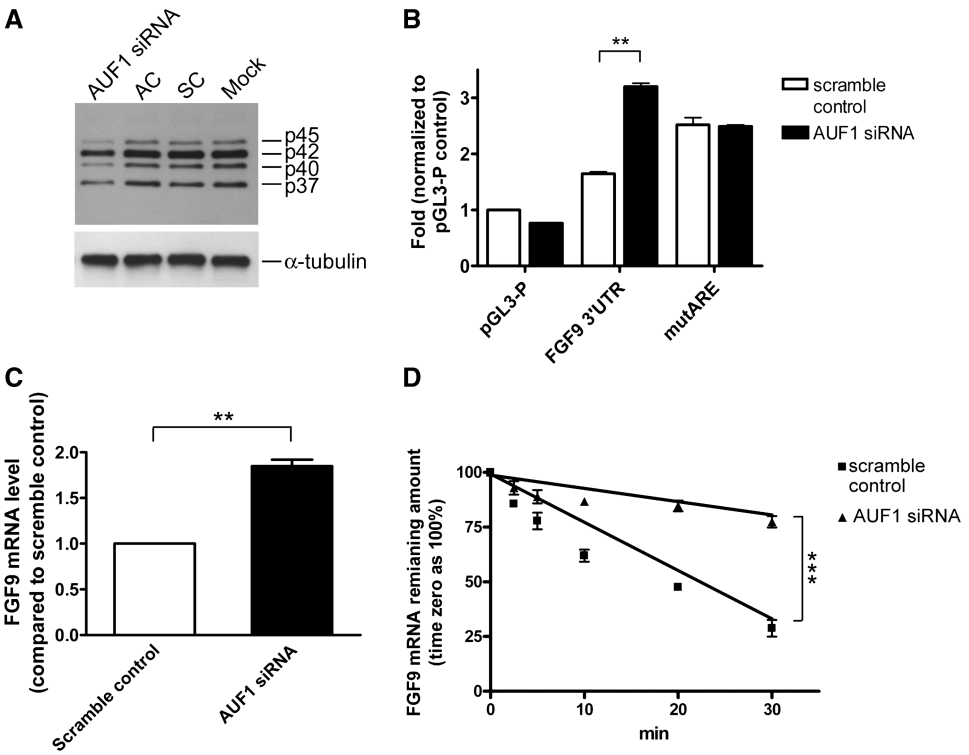

Figure 4. AUF1 controls *FGF9* mRNA stability. (**A**) Western blots showing AUF1-specific siRNA, but not the scramble control (SC) or AUF1-specific siRNA control (AC), knocks down AUF1 protein. Mock is HEK293 cells treated with transfecting reagent only and α-tubulin was used as a control. (**B**) Luciferase reporter activities in empty vector (pGL3-P), full length (FGF9 3′-UTR), and mutant (mutARE) after AUF1 or scramble siRNA knockdown were shown. (**C**) Endogenous *FGF9* mRNA levels in HEK293 cells following AUF1 or scramble siRNA knockdown. (**D**) Real-time RT-qPCR measurements showing the half-life of endogenous *FGF9* mRNA with or without siRNA knockdown. Results are normalized to time zero for each construct. All data are shown as mean ± SEM of 4–6 independent experiments. $^{**}P < 0.01$; $^{***}P < 0.001$.

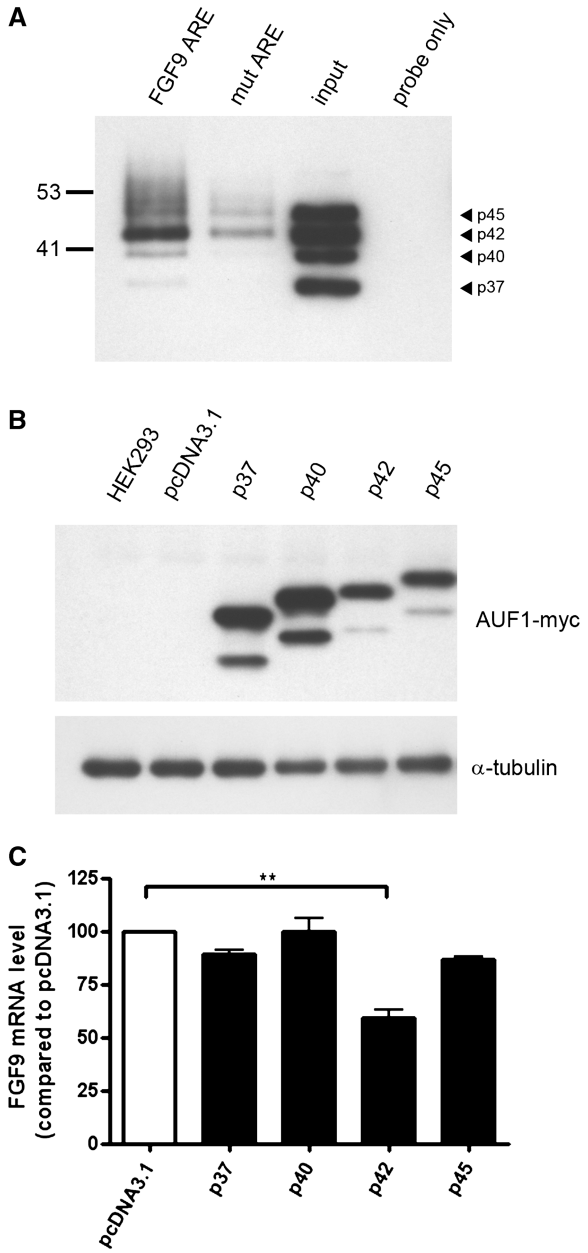

Figure 5. AUF1 p42 isoform selectively downregulates *FGF9* mRNA expression. (**A**) Pull-down assay showing that $p42^{AUF1}$ is the major isoform pulled down by biotin-labeled FGF9 ARE probe. Arrowhead indicates the position of each AUF1 isoform. Note that the mutant is markedly weaker than the wild type. Input and probe only indicate positive and negative controls. (**B**) Western blots using anti-Myc antibody showing the expression of indicated recombinant AUF1 proteins. HEK293 and pcDNA3.1 refer to cells without transfection and cells transfected with empty vector, respectively. (**C**) Endogenous FGF9 mRNA levels relative to control (pcDNA3.1) in cells overexpressing the AUF1 isoforms p37, p40, p42 and p45. $^{**}P < 0.01$.

proteins, four AUF1 isoforms were cloned and overexpressed in HEK293 cells. The expression of each isoform was confirmed by western blot analysis with anti-myc antibody (Figure 5B). Followed by RNA isolation and RT-qPCR analysis, our data showed a 50% decrease of *FGF9* mRNA in cells overexpressing $p42^{AUF1}$ ($P < 0.01$), while the other AUF1 isoforms (p37, p40 and p45) only had minor and non-significant effects on the *FGF9* mRNA level (Figure 5C). As we have demonstrated, AUF1 is involved in destabilization of human *FGF9* transcripts (Figure 4) and these data suggested that $p42^{AUF1}$ has the ability to selectively downregulate *FGF9* expression by binding to 3′-UTR ARE and destabilizing the *FGF9* transcripts.

AUF1 contributes to the regulation of PGE_2-mediated induction of *FGF9* mRNA

We previously showed that PGE_2 induces an acute and transient increase of *FGF9* mRNA in human primary endometrial stromal cells (19). We hypothesized that AUF1 is involved in the reduction of *FGF9* mRNA in stromal cells. To test this hypothesis, we knocked down AUF1 by shRNA interference in primary endometrial stromal cells. Western blot analysis revealed that the AUF1 abundance was reduced by 60–90% in primary stromal cells infected with AUF1 shRNA (Figure 6A). We then determined whether knockdown of AUF1 affects *FGF9* mRNA expression in non-stimulated cells or cells exposed to PGE_2. In agreement with previous report, administration of 1 μM PGE_2 enhanced *FGF9* mRNA by 3-fold; the level peaked at 4 h and then declined toward the basal level by 12 h ($P < 0.001$; Figure 6B). Interestingly, AUF1 knockdown caused a prolonged elevation of PGE_2-induced *FGF9* mRNA level ($P < 0.001$; Figure 6C). The *FGF9* mRNA remained elevated even at 24 h after PGE_2 treatment.

To reveal the mechanism underlying this regulation, we measured the expression of AUF1 after PGE_2 treatment in whole-cell lysates, and found that PGE_2 had no effect on AUF1 expression in primary stromal cells (Figure 6D). This suggested that other mechanisms, for example, decreased amounts of cytoplasmic AUF1 (35) or phosphorylation of AUF1 proteins (36), are involved in the regulation of PGE_2-induced excess of FGF9 mRNA. Further examination revealed that the levels of AUF1 phosphorylation were not changed in non-stimulated or PGE_2-treated cells (Supplementary Figure S2). Nevertheless, western blot data showed that PGE_2 significantly reduce AUF1 amount in the cytoplasmic fraction while no effect was detected in the control experiments (Figure 6E). Moreover, the time-dependent, PGE_2-mediated decline of cytoplasmic AUF1 showed perfect correlation with the reduction of FGF9 mRNA during the time course of this stimulation (Figure 6B and E). These results demonstrated that AUF1, through the change of its cellular distribution, plays a vital role in controlling *FGF9* mRNA level in PGE_2-induced *FGF9* transcription.

DISCUSSION

Fibroblast growth factor 9 plays numerous physiological and pathological roles in many species (37). Considering that FGF9 controls many vital functions in developmental, physiological and pathological processes, it is important to study the molecular mechanisms responsible for

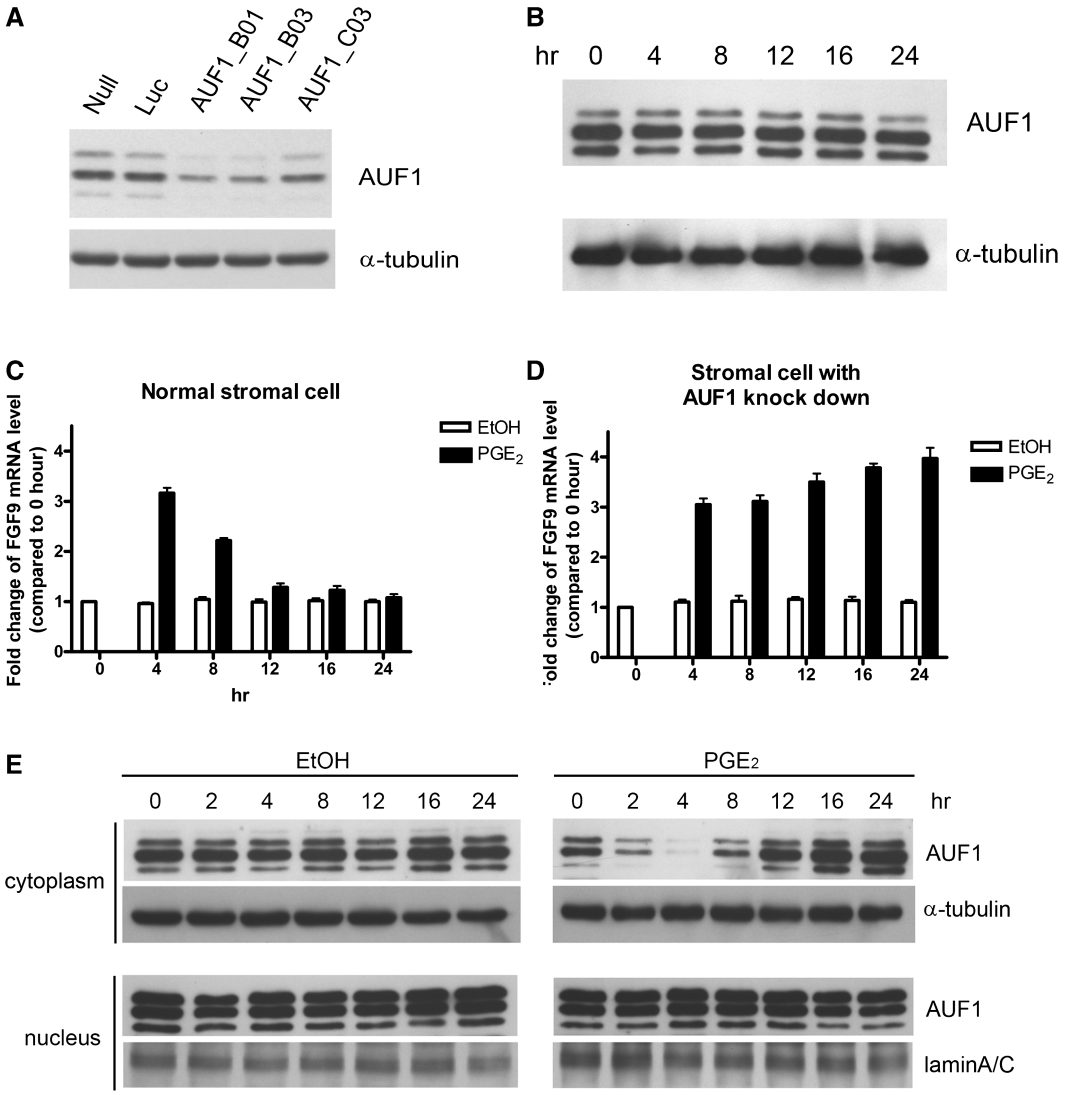

Figure 6. AUF1 knockdown sustains the PGE_2-medicated induction of *FGF9* mRNA in human primary endometrial stromal cells. (**A**) Western blots showing successful AUF1 knockdown by AUF1-specific shRNA (B01, B03 and C03), but not the Luc control shRNA. The Null indicates cells without shRNA treatment. (**B**) Western blots showing AUF1 protein expression in whole-cell lysates isolated from stromal cells after PGE_2 treatment. (**C**) *FGF9* mRNA levels measured at indicated times after PGE_2 treatment in stromal cells. Ethanol (EtOH) was used as control treatment. (**D**) Experiment similar to that shown in C, but with AUF1 knockdown by AUF1_B03 shRNA. All data are shown as mean ± SEM of 4–6 independent experiments. $*P < 0.05$; $**P < 0.01$; $***P < 0.001$. (**E**) Western blots showing the distribution pattern of AUF1 protein in stromal cells after PGE_2 treatment. α-Tubulin and LaminA/C used as loading controls for proteins isolated from cytoplasmic and nuclear fractions, respectively.

regulation of *FGF9* gene expression. Previously, we reported that PGE_2, via its EP2 receptor-mediated signaling pathway, transcriptionally upregulates *FGF9* gene expression (19). Although the data provide valuable information for understanding the regulation of *FGF9* gene expression, it cannot answer the question of why upregulation of FGF9 is transient. In this study, we showed that a nonamer AU-rich element (AUUUAUU UA) within the 3′-UTR of the *FGF9* transcript is involved in rapid mRNA turnover. RNA–protein interaction and overexpression studies revealed that $p42^{AUF1}$ is the major isoform of the AUF1 protein family that binds to *FGF9* ARE to selectively regulate the levels of *FGF9* mRNA. Our data provided direct evidence to show that AUF1 acts as a negative regulator for *FGF9* expression post-transcriptionally. To our knowledge, this is the first report to demonstrate a post-transcriptional regulation of FGF9 in any species. Our results provide the molecular and cellular mechanism underlying the homeostasis of *FGF9* mRNA level in cells, an important balance between the normal physiological function and abnormal pathological process.

We determined that the half-life of *FGF9* mRNA is <20 min, a typical characteristic of the mRNAs of tightly regulated genes, which indicates that a post-transcriptional regulatory mechanism exists to control the lifespan of *FGF9* mRNA. In addition, FGF9 is a potent peptide growth factor that stimulates the

proliferation of many cells including endometrial epithelium and stroma, prostate cancer cells and neuronal cells (19). However, these effects must be controlled during a short period of time to avoid overstimulation due to sustained elevation of FGF9. PGE_2 is a versatile eicosanoid that regulates key responses in numerous physiological and pathological processes (38). Results from the present study showed that AUF1 is able to bind and reduce *FGF9* mRNA to the basal level once it is transcriptionally activated by PGE_2. And AUF1 knockdown leads to maintained *FGF9* mRNA levels after activation. These findings indicate that AUF1 stops FGF9 signaling by destabilizing *FGF9* mRNA and thus reducing the amount of FGF9 protein synthesis. Taken together, these data also suggest that AUF1 precisely regulates FGF9 signaling by terminating the effect of environmental stimuli on FGF9. This is a very important safeguarding system to control FGF9 signaling within a precise time window or at a certain developmental stage. Therefore, loss of this control may prolong the effect of FGF9 and contribute to disease processes. Reports of other AUF1 target mRNAs from other groups are consistent with this theory. For instance, alteration of the U-rich region in the 3′-UTR of *Bcl-2* mRNA increases mRNA stability and contributes to the overproduction of the anti-apoptotic Bcl-2 protein that is responsible for the transformation of follicular B-cell lymphoma (39,40). In addition, AUF1 knockout mice display symptoms of severe endotoxic shock, including vascular hemorrhage, intravascular coagulation and high mortality, upon endotoxin challenge (41) suggesting that the lack of this negative feedback system by AUF1 indeed results in disease development and detrimental effects.

AUF1, the most extensively studied AU-rich element binding protein, is a shuttle protein (42,43) with multiple functions, such as DNA binding (44), RNA turnover (45) and mRNA translation efficiency (46). The AUF1 family contains four isoforms (p37, p40, p42 and p45) resulting from alternative splicing. Different isoforms vary significantly in their cellular distribution and binding affinity to ARE-containing mRNA. It was suggested that relative level, rather than the absolute amount of individual AUF1isoform, determine the net mRNA stability of ARE-containing transcripts (47). In this study, we showed that the p40/p42 proteins are the predominant isoforms in both HEK293 and human primary endometrial stromal cells. In addition, we have shown that p42 isoform specifically suppresses *FGF9* mRNA stability compared with the other isoforms. Our results concur with several lines of evidence that demonstrate certain transcripts are under isoform-specific regulation by the AUF1 family. For example, ectopic overexpression of the p37 isoform selectively degrades ARE-containing mRNA (42), the p45 isoform selectively binds to estrogen receptor mRNA to upregulate gene expression (48) and the p40 isoform selectively and positively regulates interleukin (IL) 10 expression in monocytes (49). Although it is known that different AUF1 isoforms have different binding affinity to specific mRNA 3′-UTRs (50,51), the detailed mechanism by which AUF1 isoforms selectively regulate *FGF9* mRNA remains unclear. In addition, a time-dependent decline in cytoplasmic AUF1 was observed along with the increase of FGF9 by PGE_2 treatment, whereas the control experiments by ethanol kept at relatively steady-state levels over the time courses. The functional significance of changing cellular distribution of AUF1 still requires further investigation. Nevertheless, similar changes in AUF1 decreasing cytoplasmic level have been associated with hydrogen peroxide (H_2O_2)-induced p16 expression (35) and in thyroid carcinoma progression (52).

The concept of RNA regulation has currently gained much attention and attempts have been made to explain the complex mechanisms of gene regulation at the post-transcription level (53). The fate of transcripts with similar functions may be under the same control mechanism, such as the PUF RNA-binding protein family (53). The *FGF* gene family members share a high degree of conservation and are involved in diverse physiological events (37). However, factors that regulate the expression of *FGFs* remain largely elusive. Previous studies show that many growth factors and signal traducers are ARE-containing transcripts in the human genome [review see (54)]. Using computational analysis (55), our data indicated that nine members of the *FGF* family (*FGF2*, *4*, *5*, *7*, *9*, *14*, *18*, *19*, *21* and *23*) are all ARE-containing genes (Supplementary Table S1). Although only *FGF9* ARE is proved to be functional and plays a vital role in *FGF9* regulation in this study, these data suggest that ARE-mediated decay is a common pathway to control expression of *FGFs*. Further, it also suggests that the ARE-mediated decay pathway is another example of RNA regulon that coordinates several physiological conditions through post-transcriptional regulation.

In summary, we have identified a novel mechanism to regulate FGF9 steady-state and stimulus-induced expression by AUF1-mediated mRNA decay. Considering that FGF9 is a potent growth and survival factor, it is not surprising that its expression is tightly controlled by many factors such as transcription factors, microsatellite motifs, and, as reported in this study, the RNA destabilizing protein, AUF1. Our findings provide a new point of view, that some diseases induced by overexpression of peptide growth factors (such as FGF9) might be due to loss-of-function of a negative regulator, for example, an RNA destabilizing protein like AUF1. Nevertheless, it is worth noting that we observed three RNA–protein complexes in the UV cross-linking assay using FGF9 ARE probe. It suggests other ARE-binding proteins may also play some roles in regulation of FGF9 mRNA stability. Among all identified ARE-binding proteins, both HuR (56) and KSRP (57) are known to interact with AUF1 and coordinately regulate ARE-containing mRNA stability. It is of interest to study whether HuR or KSRP binds to FGF9 ARE and control its expression in future investigations.

SUPPLEMENTARY DATA

Supplementary Data are available at NAR Online.

ACKNOWLEDGEMENTS

The authors would like to thank Dr Iain Bruce for the excellent help in English editing and National RNAi Core Facility, Taiwan for various RNAi constructs.

FUNDING

Funding for open access charge: National Science Council, Taiwan (NSC 98-3112-B-006-002 to H.S.S.).

Conflict of interest statement. None declared.

REFERENCES

1. Beenken,A. and Mohammadi,M. (2009) The FGF family: biology, pathophysiology and therapy. *Nat. Rev. Drug Discov.*, **8**, 235–253.
2. Goldfarb,M. (1996) Functions of fibroblast growth factors in vertebrate development. *Cytokine Growth Factor Rev.*, **7**, 311–325.
3. Gerwins,P., Skoldenberg,E. and Claesson-Welsh,L. (2000) Function of fibroblast growth factors and vascular endothelial growth factors and their receptors in angiogenesis. *Crit. Rev. Oncol. Hematol.*, **34**, 185–194.
4. Allouche,M. and Bikfalvi,A. (1995) The role of fibroblast growth factor-2 (FGF-2) in hematopoiesis. *Prog. Growth Factor Res.*, **6**, 35–48.
5. Galzie,Z., Kinsella,A.R. and Smith,J.A. (1997) Fibroblast growth factors and their receptors. *Biochem. Cell Biol.*, **75**, 669–685.
6. Song,J. and Slack,J.M. (1996) XFGF-9: a new fibroblast growth factor from Xenopus embryos. *Dev. Dyn.*, **206**, 427–436.
7. Itoh,N. and Ornitz,D.M. (2004) Evolution of the Fgf and Fgfr gene families. *Trends Genet.*, **20**, 563–569.
8. Kanda,T., Iwasaki,T., Nakamura,S., Kurokawa,T., Ikeda,K. and Mizusawa,H. (2000) Self-secretion of fibroblast growth factor-9 supports basal forebrain cholinergic neurons in an autocrine/paracrine manner. *Brain Res.*, **876**, 22–30.
9. Naruo,K., Seko,C., Kuroshima,K., Matsutani,E., Sasada,R., Kondo,T. and Kurokawa,T. (1993) Novel secretory heparin-binding factors from human glioma cells (glia-activating factors) involved in glial cell growth. Purification and biological properties. *J. Biol. Chem.*, **268**, 2857–2864.
10. Tsai,S.J., Wu,M.H., Chen,H.M., Chuang,P.C. and Wing,L.Y. (2002) Fibroblast growth factor-9 is an endometrial stromal growth factor. *Endocrinology*, **143**, 2715–2721.
11. Miyamoto,M., Naruo,K., Seko,C., Matsumoto,S., Kondo,T. and Kurokawa,T. (1993) Molecular cloning of a novel cytokine cDNA encoding the ninth member of the fibroblast growth factor family, which has a unique secretion property. *Mol. Cell Biol.*, **13**, 4251–4259.
12. Colvin,J.S., Feldman,B., Nadeau,J.H., Goldfarb,M. and Ornitz,D.M. (1999) Genomic organization and embryonic expression of the mouse fibroblast growth factor 9 gene. *Dev. Dyn.*, **216**, 72–88.
13. Hendrix,N.D., Wu,R., Kuick,R., Schwartz,D.R., Fearon,E.R. and Cho,K.R. (2006) Fibroblast growth factor 9 has oncogenic activity and is a downstream target of Wnt signaling in ovarian endometrioid adenocarcinomas. *Cancer Res.*, **66**, 1354–1362.
14. Kathpalia,V.P., Mussak,E.N., Chow,S.S., Lam,P.H., Skelley,N., Time,M., Markelewicz,R.J. Jr, Kanduc,D., Lomas,L., Xiang,Z. *et al.* (2006) Genome-wide transcriptional profiling in human squamous cell carcinoma of the skin identifies unique tumor-associated signatures. *J. Dermatol.*, **33**, 309–318.
15. Wing,L.Y., Chuang,P.C., Wu,M.H., Chen,H.M. and Tsai,S.J. (2003) Expression and mitogenic effect of fibroblast growth factor-9 in human endometriotic implant is regulated by aberrant production of estrogen. *J. Clin. Endocrinol. Metab.*, **88**, 5547–5554.
16. Huang,J.Y., Hong,Y.T. and Chuang,J.I. (2009) Fibroblast growth factor 9 prevents MPP+-induced death of dopaminergic neurons and is involved in melatonin neuroprotection *in vivo* and *in vitro*. *J. Neurochem.*, **109**, 1400–1412.
17. Chen,T.M., Kuo,P.L., Hsu,C.H., Tsai,S.J., Chen,M.J., Lin,C.W. and Sun,H.S. (2007) Microsatellite in the 3′ untranslated region of human fibroblast growth factor 9 (FGF9) gene exhibits pleiotropic effect on modulating FGF9 protein expression. *Hum. Mutat.*, **28**, 98.
18. Lin,Y.M., Tsai,C.C., Chung,C.L., Chen,P.R., Sunny Sun,H., Tsai,S.J. and Huang,B.M. (2010) Fibroblast growth factor 9 stimulates steroidogenesis in postnatal Leydig cells. *Int. J. Androl*, **33**, 545–553.
19. Chuang,P.C., Sun,H.S., Chen,T.M. and Tsai,S.J. (2006) Prostaglandin E2 induces fibroblast growth factor 9 via EP3-dependent protein kinase Cdelta and Elk-1 signaling. *Mol. Cell Biol.*, **26**, 8281–8292.
20. Giri,D., Ropiquet,F. and Ittmann,M. (1999) FGF9 is an autocrine and paracrine prostatic growth factor expressed by prostatic stromal cells. *J. Cell Physiol.*, **180**, 53–60.
21. Seo,M. and Noguchi,K. (1995) Retinoic acid induces gene expression of fibroblast growth factor-9 during induction of neuronal differentiation of mouse embryonal carcinoma P19 cells. *FEBS Lett.*, **370**, 231–235.
22. Ross,J. (1996) Control of messenger RNA stability in higher eukaryotes. *Trends Genet.*, **12**, 171–175.
23. Chen,C.Y. and Shyu,A.B. (1995) AU-rich elements: characterization and importance in mRNA degradation. *Trends Biochem. Sci.*, **20**, 465–470.
24. Xu,N., Chen,C.Y. and Shyu,A.B. (1997) Modulation of the fate of cytoplasmic mRNA by AU-rich elements: key sequence features controlling mRNA deadenylation and decay. *Mol. Cell Biol.*, **17**, 4611–4621.
25. Wilson,T. and Treisman,R. (1988) Removal of poly(A) and consequent degradation of c-fos mRNA facilitated by 3′ AU-rich sequences. *Nature*, **336**, 396–399.
26. Wu,M.H., Shoji,Y., Chuang,P.C. and Tsai,S.J. (2007) Endometriosis: disease pathophysiology and the role of prostaglandins. *Expert Rev. Mol. Med.*, **9**, 1–20.
27. Chen,C.Y., Xu,N. and Shyu,A.B. (1995) mRNA decay mediated by two distinct AU-rich elements from c-fos and granulocyte-macrophage colony-stimulating factor transcripts: different deadenylation kinetics and uncoupling from translation. *Mol. Cell Biol.*, **15**, 5777–5788.
28. Bevilacqua,A., Ceriani,M.C., Capaccioli,S. and Nicolin,A. (2003) Post-transcriptional regulation of gene expression by degradation of messenger RNAs. *J. Cell Physiol.*, **195**, 356–372.
29. Zhang,W., Wagner,B.J., Ehrenman,K., Schaefer,A.W., DeMaria,C.T., Crater,D., DeHaven,K., Long,L. and Brewer,G. (1993) Purification, characterization, and cDNA cloning of an AU-rich element RNA-binding protein, AUF1. *Mol. Cell Biol.*, **13**, 7652–7665.
30. Lai,W.S., Kennington,E.A. and Blackshear,P.J. (2003) Tristetraprolin and its family members can promote the cell-free deadenylation of AU-rich element-containing mRNAs by poly(A) ribonuclease. *Mol. Cell Biol.*, **23**, 3798–3812.
31. Gherzi,R., Lee,K.Y., Briata,P., Wegmuller,D., Moroni,C., Karin,M. and Chen,C.Y. (2004) A KH domain RNA binding protein, KSRP, promotes ARE-directed mRNA turnover by recruiting the degradation machinery. *Mol. Cell*, **14**, 571–583.
32. Ale-Agha,N., Galban,S., Sobieroy,C., Abdelmohsen,K., Gorospe,M., Sies,H. and Klotz,L.O. (2009) HuR regulates gap junctional intercellular communication by controlling beta-catenin levels and adherens junction integrity. *Hepatology*, **50**, 1567–1576.
33. Mignone,F., Grillo,G., Licciulli,F., Iacono,M., Liuni,S., Kersey,P.J., Duarte,J., Saccone,C. and Pesole,G. (2005) UTRdb and UTRsite: a collection of sequences and regulatory motifs of the untranslated regions of eukaryotic mRNAs. *Nucleic Acids Res.*, **33**, D141–D146.
34. Mignone,F., Gissi,C., Liuni,S. and Pesole,G. (2002) Untranslated regions of mRNAs. *Genome Biol.*, **3**, REVIEWS0004.
35. Guo,G.E., Ma,L.W., Jiang,B., Yi,J., Tong,T.J. and Wang,W.G. (2010) Hydrogen peroxide induces p16(INK4a) through an AUF1-dependent manner. *J. Cell Biochem.*, **109**, 1000–1005.
36. Wilson,G.M., Lu,J., Sutphen,K., Sun,Y., Huynh,Y. and Brewer,G. (2003) Regulation of A + U-rich element-directed mRNA turnover involving reversible phosphorylation of AUF1. *J. Biol. Chem.*, **278**, 33029–33038.

37. Itoh,N. and Ornitz,D.M. (2008) Functional evolutionary history of the mouse Fgf gene family. *Dev. Dyn.*, **237**, 18–27.
38. Park,J.Y., Pillinger,M.H. and Abramson,S.B. (2006) Prostaglandin E2 synthesis and secretion: the role of PGE2 synthases. *Clin. Immunol.*, **119**, 229–240.
39. Lapucci,A., Donnini,M., Papucci,L., Witort,E., Tempestini,A., Bevilacqua,A., Nicolin,A., Brewer,G., Schiavone,N. and Capaccioli,S. (2002) AUF1 Is a bcl-2 A + U-rich element-binding protein involved in bcl-2 mRNA destabilization during apoptosis. *J. Biol. Chem.*, **277**, 16139–16146.
40. Shchors,K., Yehiely,F., Kular,R.K., Kotlo,K.U., Brewer,G. and Deiss,L.P. (2002) Cell death inhibiting RNA (CDIR) derived from a 3′-untranslated region binds AUF1 and heat shock protein 27. *J. Biol. Chem.*, **277**, 47061–47072.
41. Lu,J.Y., Sadri,N. and Schneider,R.J. (2006) Endotoxic shock in AUF1 knockout mice mediated by failure to degrade proinflammatory cytokine mRNAs. *Genes Dev.*, **20**, 3174–3184.
42. Sarkar,B., Lu,J.Y. and Schneider,R.J. (2003) Nuclear import and export functions in the different isoforms of the AUF1/heterogeneous nuclear ribonucleoprotein protein family. *J. Biol. Chem.*, **278**, 20700–20707.
43. Chen,C.Y., Xu,N., Zhu,W. and Shyu,A.B. (2004) Functional dissection of hnRNP D suggests that nuclear import is required before hnRNP D can modulate mRNA turnover in the cytoplasm. *RNA*, **10**, 669–680.
44. Enokizono,Y., Konishi,Y., Nagata,K., Ouhashi,K., Uesugi,S., Ishikawa,F. and Katahira,M. (2005) Structure of hnRNP D complexed with single-stranded telomere DNA and unfolding of the quadruplex by heterogeneous nuclear ribonucleoprotein D. *J. Biol. Chem.*, **280**, 18862–18870.
45. DeMaria,C.T. and Brewer,G. (1996) AUF1 binding affinity to A+U-rich elements correlates with rapid mRNA degradation. *J. Biol. Chem.*, **271**, 12179–12184.
46. Liao,B., Hu,Y. and Brewer,G. (2007) Competitive binding of AUF1 and TIAR to MYC mRNA controls its translation. *Nat. Struct. Mol. Biol.*, **14**, 511–518.
47. Raineri,I., Wegmueller,D., Gross,B., Certa,U. and Moroni,C. (2004) Roles of AUF1 isoforms, HuR and BRF1 in ARE-dependent mRNA turnover studied by RNA interference. *Nucleic Acids Res.*, **32**, 1279–1288.
48. Ing,N.H., Massuto,D.A. and Jaeger,L.A. (2008) Estradiol up-regulates AUF1p45 binding to stabilizing regions within the 3′-untranslated region of estrogen receptor alpha mRNA. *J. Biol. Chem.*, **283**, 1764–1772.
49. Sarkar,S., Sinsimer,K.S., Foster,R.L., Brewer,G. and Pestka,S. (2008) AUF1 isoform-specific regulation of anti-inflammatory IL10 expression in monocytes. *J. Interferon. Cytokine Res.*, **28**, 679–691.
50. Wagner,B.J., DeMaria,C.T., Sun,Y., Wilson,G.M. and Brewer,G. (1998) Structure and genomic organization of the human AUF1 gene: alternative pre-mRNA splicing generates four protein isoforms. *Genomics*, **48**, 195–202.
51. Kajita,Y., Nakayama,J., Aizawa,M. and Ishikawa,F. (1995) The UUAG-specific RNA binding protein, heterogeneous nuclear ribonucleoprotein D0. Common modular structure and binding properties of the 2xRBD-Gly family. *J. Biol. Chem.*, **270**, 22167–22175.
52. Trojanowicz,B., Brodauf,L., Sekulla,C., Lorenz,K., Finke,R., Dralle,H. and Hoang-Vu,C. (2009) The role of AUF1 in thyroid carcinoma progression. *Endocr. Relat. Cancer*, **16**, 857–871.
53. Keene,J.D. (2007) RNA regulons: coordination of post-transcriptional events. *Nat. Rev. Genet.*, **8**, 533–543.
54. Barreau,C., Paillard,L. and Osborne,H.B. (2005) AU-rich elements and associated factors: are there unifying principles? *Nucleic Acids Res.*, **33**, 7138–7150.
55. Halees,A.S., El-Badrawi,R. and Khabar,K.S. (2008) ARED Organism: expansion of ARED reveals AU-rich element cluster variations between human and mouse. *Nucleic Acids Res.*, **36**, D137–D140.
56. Pan,Y.X., Chen,H. and Kilberg,M.S. (2005) Interaction of RNA-binding proteins HuR and AUF1 with the human ATF3 mRNA 3′-untranslated region regulates its amino acid limitation-induced stabilization. *J. Biol. Chem.*, **280**, 34609–34616.
57. Nechama,M., Ben-Dov,I.Z., Briata,P., Gherzi,R. and Naveh-Many,T. (2008) The mRNA decay promoting factor K-homology splicing regulator protein post-transcriptionally determines parathyroid hormone mRNA levels. *FASEB J.*, **22**, 3458–3468.